communications earth & environment

Article

https://doi.org/10.1038/s43247-024-01253-6

Future transition from forests to shrublands and grasslands in the western United States is expected to reduce carbon storage

Check for updates

Jared M. Kodero [1,2] ✉, Benjamin S. Felzer [1] & Yuning Shi[3]

Climate change is expected to impact vegetation in the western United States, leading to shifts in dominant Plant Functional Types and carbon storage. Here, we used a biogeographic model integrated with a biogeochemical model to predict changes in dominant Plant Functional Type by 2070−2100. Results show that under the Representative Concentration Pathway 4.5 scenario, 40% of the originally forested areas will transition to shrubland (7%) or grassland (32%), while under the Representative Concentration Pathway 8.5 scenario, 58% of forested areas shift to shrubland (18%) or grassland (40%). These shifts in Plant Functional Types result in a net overall loss in carbon storage equal to −60 gigagram of carbon and −82 gigagram of carbon under Representative Concentration Pathway 4.5 and 8.5, respectively. Our findings highlight the need for urgent action to mitigate the effects of climate change on vegetation and carbon storage in the region.

Forests in the western United States are likely to transition to shrubland or grassland vegetation types or be replaced by forest communities better adapted to fires and droughts and thrive in warmer climates[1–3]. Recent research has highlighted an increase in drought intensity, fire frequency, and burn severity in the region. These changes are complexly intertwined and are primarily driven by climate change caused by anthropogenic emissions of greenhouse gases[4,5]. Burn severity is further exacerbated by historical fire deficit that led to fuel accumulation, which causes fires to be more severe when they occur.

Sample pollen analyses show that historical climate changes in the region resulted in vegetation shifts[6,7]. Other studies also show that following the end of the last glacial period, vegetation in the western United States exhibited individualistic responses to warming, which affected species range and distribution. Because this warming was gradual, plant species had enough time to disperse and find new suitable habitats[8]. However, unlike in the past, the current rate of warming, frequency of wildfires, and increased burn severity may not give forest communities enough time to adapt, resulting in climate-vegetation mismatch.

Changes in dominant plant functional types (PFTs) will most likely be driven by increased fires exacerbated by historical fuel accumulation, persistent droughts, and warming. PFT's response to these changes will depend on their physiological tolerance, phenology, fire adaptation, and how different PFTs compete[9,10].

While historical fires mediated the response of forests to climate change by accelerating species turnovers or selecting fire-adapted species[11], these adaptations are specific to particular mild to moderate fire regimes. Forests not adapted to high-severity stand-replacing fires, therefore, may respond in ways that are challenging to predict and have no historical precedent[12]. Increased stand-replacing fires clear forests and remove seed sources from forest types not already adapted to them, allowing grasses or shrubs to expand in habitats previously dominated by tree PFTs[13].

Future climate projections for the western United States show continued warming and increased droughts due to altered precipitation patterns. The resulting environmental stress will promote PFT alteration as younger seedlings are sensitive to changes in temperature and precipitation patterns. Some modeling studies project a complete transition from forest to shrubland or grasslands[14–16], while others suggest only shifts in dominant forest species[17]. By the end of the century, it is projected that 55% of future landscapes in the western United States will have climates incompatible with the vegetation communities that now occur on those landscapes[18].

Here, we developed a biogeography module based on BIOME4[19,20]—a biogeography model that simulates the equilibrium distribution of

[1]Lehigh University, Bethlehem, PA, USA. [2]Brown University, Providence, RI, USA. [3]The Pennsylvania State University, University Park, PA, USA.
✉e-mail: jared_kodero@brown.edu

dominant PFTs integrated within an existing biogeochemical model[21]. We then used the resulting model to assess the impact of changing climate on dominant PFTs in forested regions of the western United States, where trees are the dominant PFTs and determined whether these changes will result in a shift in the dominant PFTs under Representative Concentration Pathway (RCP) 4.5 and 8.5 at a monthly time step. The model uses bioclimatic envelopes to determine the PFTs that can exist in each grid cell. PFT competition is based on total Net Primary Productivity (NPP), where the most productive PFT is considered the dominant PFT, which is then selected and given 100% coverage of the grid cell. Each grid cell is 0.5 by 0.5 degrees. In our future run (2015–2100), we simulate varying levels of fire severity governed by ignition, fuel availability, and fuel combustibility. Historical fires use the same fire module but are modified to better capture historical fire regimes, as described in the Online Methods section. Analysis of model results focuses on changes occurring by the end of the century 2070–2100.

Results

Change in dominant PFT

Under the RCP 4.5 scenario, our model predicts that 40% of grids originally dominated by tree PFTs during the 1984–2014 period will transition to shrubs (7%) and grass (32%) by the end of the century. In contrast, under RCP 8.5, 58% will transition to shrub (18%) or grass (40%) as the dominant PFT (Figs. 1 and 2).

Shifts predominantly occur in grids projected to experience the greatest temperature rise and decreased soil moisture, associated with severe, stand-replacing fires. Principal Component analysis under RCP 4.5 indicates that 55% of the variance is due to moisture stress, 27% to fires, 13% to temperature, and 6% to total precipitation. For RCP 8.5, the Principal Component analysis loadings are 53%, 26%, 14%, and 7%, respectively. The four variables tested are interrelated: warming worsens drought, leading to more severe fires that clear tree PFTs, allowing grass and shrub expansion[22]. These findings highlight the roles of temperature, moisture stress, and fire severity in ecosystem shifts under evolving climatic scenarios. Our results show that warming and droughts lead to more severe fires (Supplementary Figs. 1 and 2).

Geographically, the most pronounced shifts from forests to grasslands are observed in the Northern Rockies and Puget Trough, while transitions from forests to shrublands are predominant in the Southwest. Additionally, our model indicates an upslope shift in the mean elevation of boreal and temperate coniferous forests under both climate scenarios (Fig. 3). This trend indicates PFTs' adaptive response to warmer and drier conditions.

The model also shows PFT's mean elevation, especially for boreal and temperate coniferous forests, shifting upslope (Fig. 3) under both scenarios by the end of the century. These shifts are expected to accelerate as the climate warms, droughts intensify, and severe fires increase.

Changes in carbon stocks and fluxes

In the model, NPP represents the difference between Gross Primary Production (GPP) and carbon loss due to respiration. NPP is primarily driven by climatic factors with tree PFTs, given optimal climatic conditions, exhibiting higher NPP compared to grass and shrub PFTs. Conversely, Net Ecosystem Productivity (NEP) is a measure of the net carbon fluxes between an ecosystem and the atmosphere, considering not only the plant carbon dynamics but also the carbon emissions from soil and other ecosystem components through heterotrophic respiration and decomposition processes. Thus, while NPP focuses on plant growth and carbon accumulation, NEP reflects the overall carbon balance of the entire ecosystem. In this study, NPP serves as an indicator of competitive success among PFTs. Vegetation and soil organic carbon are key variables as they represent the amount of carbon stored in live vegetation and the soil, respectively.

The modeled shift in dominant PFT, as depicted in Figs. 1 and 2, indicate a decrease in total NPP, vegetation carbon, and soil organic carbon by the end of the century (2070–2100) compared to the historical period (1984–2014) in both RCP 4.5 and RCP 8.5 scenarios (Fig. 4). This decline is primarily attributed to fires and unfavorable climatic conditions, which have enabled grass and shrub PFTs to expand at the expense of tree PFTs. This expansion has led to a reduction in NPP for tree PFTs. The decline in NPP for tree types is further explained by changes in climatic conditions and increased fires that favor the expansion of grass and shrub types. Furthermore, the adaptive expansion of non-forest vegetation, coupled with increased fires, has resulted in a substantial projected areal decrease of forest-to-non-forest conversion, which has substantial implications for the carbon budget. However, NEP shows an increase of up to 0.5 PgC per 30 years under RCP 8.5 and 0.2 PgC per 30 years under RCP 4.5. This increase is primarily due to more grass and shrub PFTs, suggesting their ability to thrive in warmer, drier climates and expand into areas previously dominated by tree PFTs. This shift indicates a substantial change in the regional carbon sequestration pattern, driven by changing climate and fire regimes.

The total cumulative Net Carbon Exchange (NCE) (Fig. 5), which accounts for the carbon lost during land-use conversion and products from conversion, shows a net carbon loss for the western United States equal to −60 GgC for RCP 4.5 and −82 GgC for RCP 8.5 scenario. In both scenarios, temperate coniferous forests contribute the most to the loss (Fig. 2). For NCE, carbon uptake is denoted as positive, and carbon release is denoted as

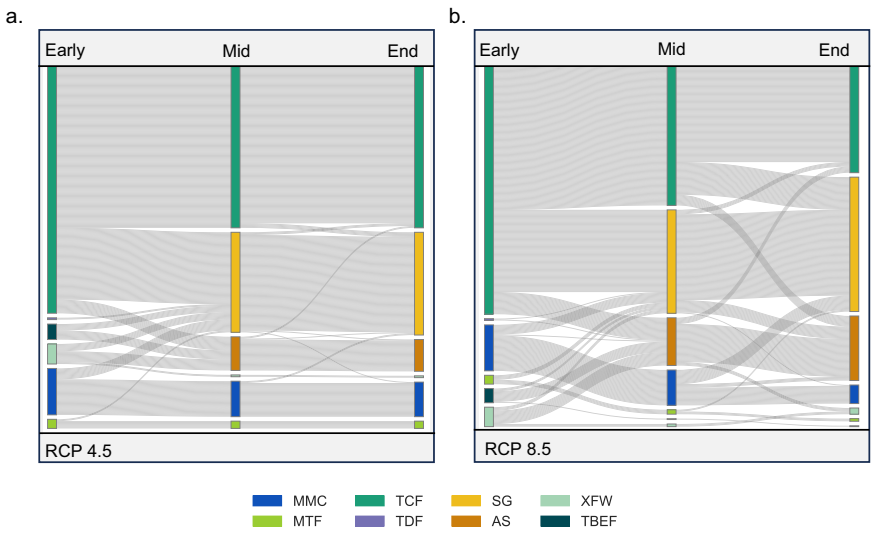

Fig. 1 | Types of shifts in dominant plant functional types in the western United States for the Early Century (1984–2014), Mid Century, and End Century (2070–2100). a Under RCP 4.5 scenario. **b** Under RCP 8.5 scenario. PFTs include MMC Mesic Mixed Coniferous Forest, MTF Mixed Temperate Forests, TDF Temperate Deciduous Forest, TCF Temperate Coniferous Forest, SG Short Grasslands, AS Arid Shrublands, XFW Xeromorphic Forests and Woodlands, TBEF Temperate Broadleaved Evergreen Forests.

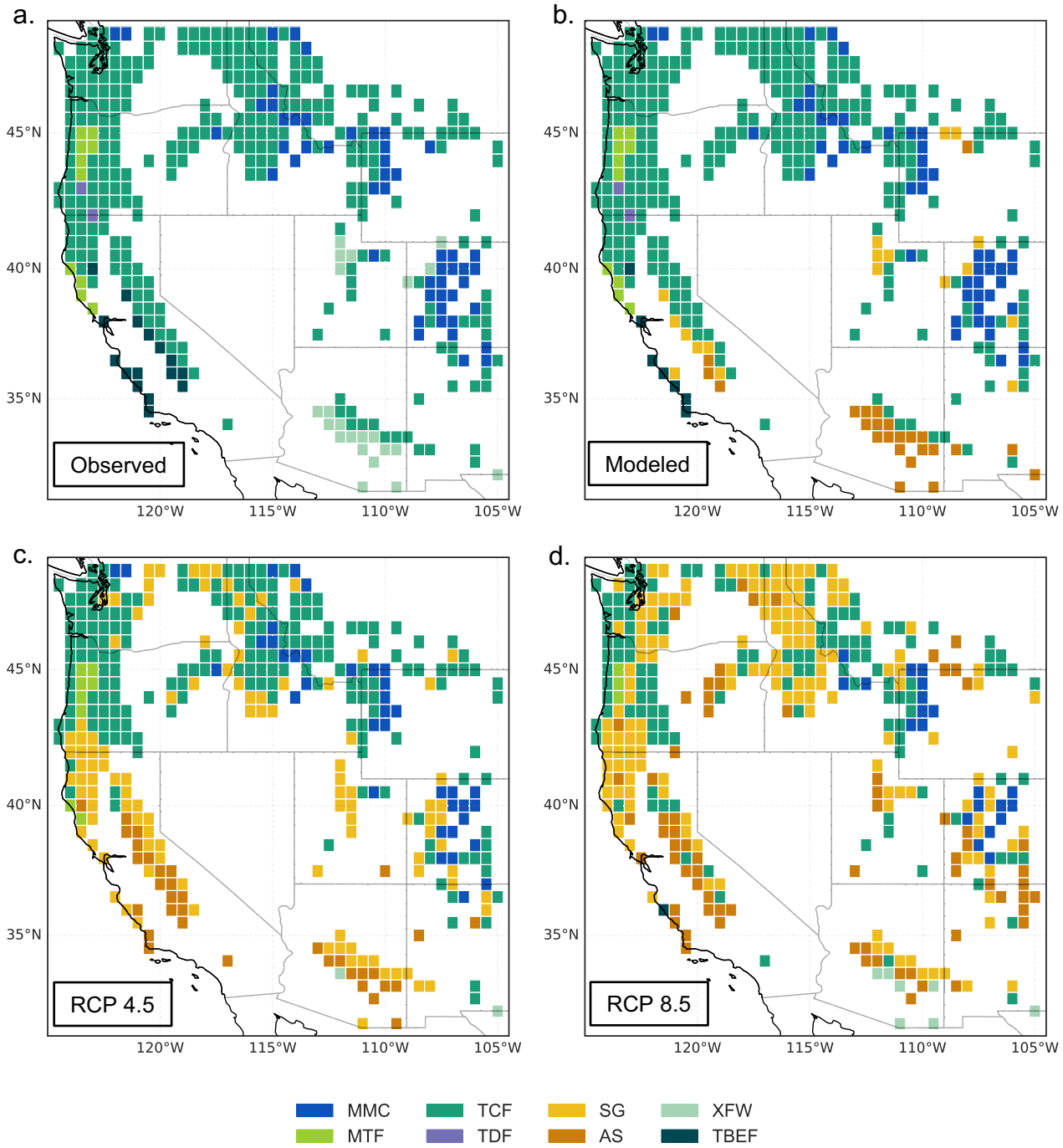

Fig. 2 | Distribution of dominant PFTs. a Observed dominant PFTs for 1984–2014. **b** Modeled dominant PFTs for 1984–2014 at a 0.5 by 0.5 deg resolution. **c** Modeled dominant PFTs for the end of the century (2070–2100) under RCP 4.5 scenario. **d** Modeled dominant PFTs for end of the century (2070–2100) under RCP 8.5 scenario. PFTs are defined in Fig. 1.

negative. NCE is calculated based on the equations below.

$$NCE = NEP - E_c \quad (1)$$

$$NEP = NPP - r_h - VOLAC \quad (2)$$

Where NCE is Net Carbon Exchange, NEP is Net Ecosystem Productivity, E_c is burned carbon, NPP is Net Primary Productivity, r_h is heterotrophic respiration, and VOLAC is the proportion of standing dead that decomposes and volatizes CO_2 directly back to the atmosphere. In this study, we excluded other conversion fluxes, i.e., decay of agricultural and wood products from NEP and NCE calculations because human land use and land cover change are not considered. The NCE we calculate is equivalent to Net Biome Productivity, which is a measure of the balance between NPP and carbon losses due to heterotrophic respiration and wildfire.

The continuous decrease in vegetation carbon and soil organic carbon trends is attributed to the increasing number of fires and decreasing coverage of tree PFTs. The increasing number of fires is a result of droughts caused by changing climatic conditions[2], effectively clearing forests, reducing biomass, and allowing grass and shrub PFTs to become dominant. In hotter and drier grids where grasses are dominant, we have more fires since grasses frequently burn more than forests (Supplementary Fig. 2). Both

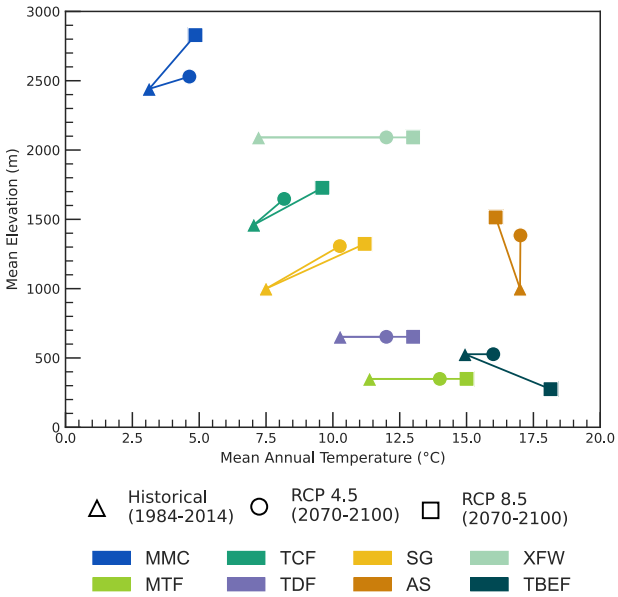

Fig. 3 | Change in dominant PFTs mean elevation and mean annual temperature by the end of the century. Comparative analysis of mean elevation and mean annual temperature changes for dominant PFTs by 2070–2100 compared to the 1984–2014 baseline under RCP 4.5 and 8.5 scenarios. PFTs are defined in Fig. 1.

scenarios show similar trends for vegetation carbon and soil organic carbon, although under RCP 8.5, we see a much higher loss of carbon, leading to a rapid decline in the total carbon stored in these ecosystems. Overall, the shift from forests to grasses and shrubs results in a loss of carbon from the land and less vegetation productivity.

Discussion

Our results project a shift in dominant PFTs from tree to grass or shrub PFTs in the western United States by the end of the century due to fire and climate change under RCP 4.5 and 8.5. This shift will be primarily driven by the increasing severity of droughts, fires, and increase in temperature. Even though climate models project increases in absolute precipitation, they are ultimately offset by changes in form and timing, especially in the intermountain region, where there is a projected shift from snow to rain[23,24]. Snow is projected to melt earlier in the spring, and most snow melt will be lost as surface runoff[25]. The remaining soil moisture may become severely depleted during the drier summer months, leaving forests moisture-stressed and vulnerable to severe fires.

The transition from tree-dominated PFTs to shrub and grass PFTs, predominantly in the northern states and Southwest region, marks a critical alteration in the ecosystem's capacity to store carbon. Under both scenarios, the decrease in NPP, vegetation carbon, and soil organic carbon is an indicator of these ecosystems' diminished carbon storage potential. Forests are known for their higher carbon storage capacity compared to shrub or grass-dominated landscapes. This shift, therefore, implies a reduction in the total carbon stocks within these regions. While NEP shows a notable increase, primarily attributed to grass and shrub PFTs, this does not entirely offset the loss in carbon storage potential due to the decrease in tree PFTs. The increased NEP is a response to the changing composition of PFTs and is not necessarily indicative of enhanced ecosystem carbon sequestration capacity. Therefore, while the NEP increases due to the expansion of grassland and shrubland, the overall carbon storage capacity (NCE) decreases due to the loss of carbon pools associated with the declining coverage of tree PFTs as a result of fires.

The altered carbon dynamics are primarily driven by a shift in PFT distribution. This shift is marked by an expansion of grass and shrub PFTs at the expense of tree PFT, particularly temperate conifers that are currently prevalent in western United States forests. As a result, there is an overall decline in total carbon storage for the whole region (Fig. 4). The elevation and range shifts (Fig. 3) suggest an adaptive response of ecosystems to the changing climate, with forests persisting in cooler and wetter regions. However, this pattern also indicates a potential narrowing of suitable habitats for tree PFT, which are crucial for high-carbon storage. The shift to shrub and grass PFTs in lower elevation and warmer areas, although contributing to an increase in NEP, may not sustain long-term carbon storage equivalent to that of forested areas.

These findings are similar to other modeling studies but slightly differ from previous studies in Yellowstone and the intermountain region[11,12], which predicted a complete change in dominant PFTs and a transition to more drought- and fire-tolerant tree species, respectively. Although we did not parameterize the model to species level, our results show that these forests persist (Figs. 1 and 2). Observational studies from networks like LTER and Carbon Flux Tower support the trends in NPP and NEP (Fig. 5), with variations across regions. One study[26] observed an increase in the annual mean NEP in temperate deciduous broadleaf forests in the western United States during 1997–2005, which declined in a subsequent warming slowdown, indicating the impact of temperature and water availability. Another study[27] reported a decrease in carbon storage in California's ecosystems from 2001 to 2100, primarily driven by climate changes and land-use alterations. Notably, decreases in NPP or NEP were typically observed in drought-affected regions. However, it's important to note that in regions where severe future droughts are expected to become more common, historical data may not yet reflect similar reductions in ecosystem carbon dynamics, as there is no historical or modern analog for such droughts[28].

Fires also play an important role in facilitating changes in dominant PFTs. In our model, ~26% of the change in dominant PFTs in both scenarios is explained by fires. Fires help facilitate the shift in dominant PFTs by clearing present vegetation in a grid cell, allowing other PFTs to establish and dominate. Moreover, fires accelerate range shifts in areas where climate-vegetation mismatches exist by affecting the rate of vegetation redistribution and increasing the seedling-only range displacement for some tree species, resulting in seedlings growing in different climatic conditions than mature trees[29]. In addition, studies have found that high fire severity and low seed availability reduce the probability of post-fire regeneration, as seen in the decline in post-fire conifer recruitment in the western United States[30]. Moreover, following stand-replacing fires, forests in the West showed little to no post-fire tree regeneration in the past two decades due to seed source limitations[31,32]. Our model does not consider these seed sources and distribution processes, as we assume that at least tree, grass, and shrub seeds are available everywhere following fires.

Forest succession following fire varies in the western United States[33]. If the climate is favorable, saplings of the same forest species are established; in some cases, different tree species may be established instead. For example, the lodgepole pine forests of the Intermountain West are homogeneous, whereas the fir-spruce-mountain hemlock group of the West Coast is not. However, our model only looks at vegetation at the PFT level, as same-tree PFTs return if the climate is favorable.

Our modeling results also agree with ongoing and modeled vegetation shifts in the Southwest and Great Plains, as seen in changes from mixed conifers to shrublands in Devil's Postpile, California, and similar transformations in Gila and Coronado National Forests[22,32,34]. These shifts, primarily driven by high-severity fires, are further exacerbated by droughts impacting vegetation mortality and warming influencing seedling growth. Recent trends show a shift from tree-dominant to non-tree-dominant vegetation due to increased burn severity, warming, and droughts. Particularly in Yellowstone, the lower montane tree cover is vulnerable to prolonged non-forest conditions if impacted by stand-replacing fires[35]. The Las Conchas fire study in New Mexico illustrates this trend, where initial burns led to transitions from forests to savannas and shrublands[29,36], which then showed greater fire resistance. Additionally, persistent droughts and rising temperatures are driving vegetation upslope across western United States mountain ranges[37]. This lag in vegetation adaptation to climate change reduces habitats and increases extinction risks for certain species.

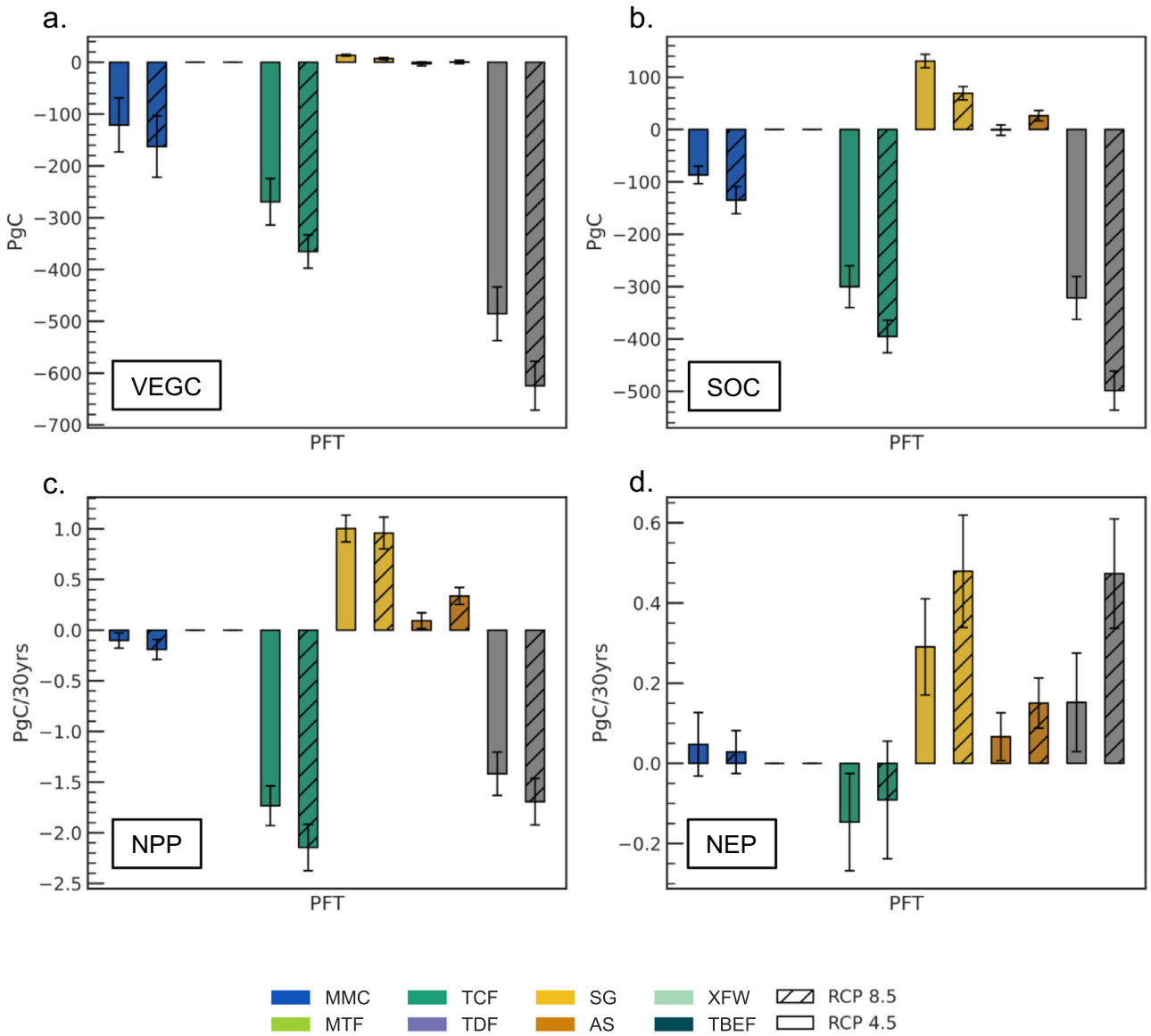

Fig. 4 | Absolute change in carbon stocks and fluxes for PFTs (2070–2100). **a** Vegetation carbon (VEGC). **b** Soil organic carbon (SOC). **c** Net primary productivity (NPP). **d** Net ecosystem productivity (NEP). Error bars represent standard deviation based on 20-models aggregation. All PFTs are statistically significant (p value < 0.05). PFTs are defined in Fig. 1.

Similar to our model results, a modeling study examining historical and future fire regimes under a changing climate in the Sierra Nevada identified a moisture threshold beyond which forests may shift to shrublands and grasslands in warmer, drier conditions[38]. It revealed a potential threshold where shifts in vegetation from forest to shrubland and grassland are possible as the climate becomes warmer and drier along the Sierra Nevada. Similarly, another study highlighted the increased risk of cheatgrass (Bromus tectorum) invasion in the western United States due to climate-induced decreases in soil moisture, predicting up to a 45% increase in suitable invasion areas across Montana, Wyoming, Utah, and Colorado[39].

These findings confirm that climate-driven shifts are ongoing, with high-severity wildfires exacerbating the decline of mature trees and unfavorable climates hindering new seedling survival. Our future model run (2015–2100), incorporating varying fire severities influenced by fuel availability and combustibility, indicates notable effects on carbon stocks and fluxes. By the century's end, there is a marked decrease in carbon storage and a rise in grass and shrub PFTs. Post-wildfire tree regeneration faces numerous climate change-related challenges, notably moisture stress. Hot, dry post-fire conditions can critically limit tree regeneration, potentially shifting landscapes towards non-tree vegetation. Factors like seed source proximity, burn severity, repeated disturbances, topographic conditions, and competition from shrubs and grasses[39] further impede tree regrowth. Although not all vegetation burns during a fire, the regrowth of trees is hindered by external environmental conditions affecting their ability to regenerate effectively following a fire.

Ecologically, forests provide essential services, including carbon sequestration and biodiversity conservation. Our models suggest that continued warming trends may shift forests to grasslands or shrublands, affecting these services. This necessitates proactive forest conservation strategies, such as fuel reduction treatments, prescribed burning, fire breaks, and planting climate-adapted trees, to mitigate wildfire impacts and adapt to changing conditions[40–42]. Post-fire reforestation can also enhance recovery, biodiversity, and carbon storage. The focus should shift to maintaining these ecosystems in areas already transitioning to grassland or shrubland. Instead of restoring the original forest, which may not be possible due to climate-vegetation mismatch, the focus should shift to maintaining these ecosystems. The findings of this study highlight the importance of targeted forest, shrubland, and grassland management and adaptation strategies to mitigate

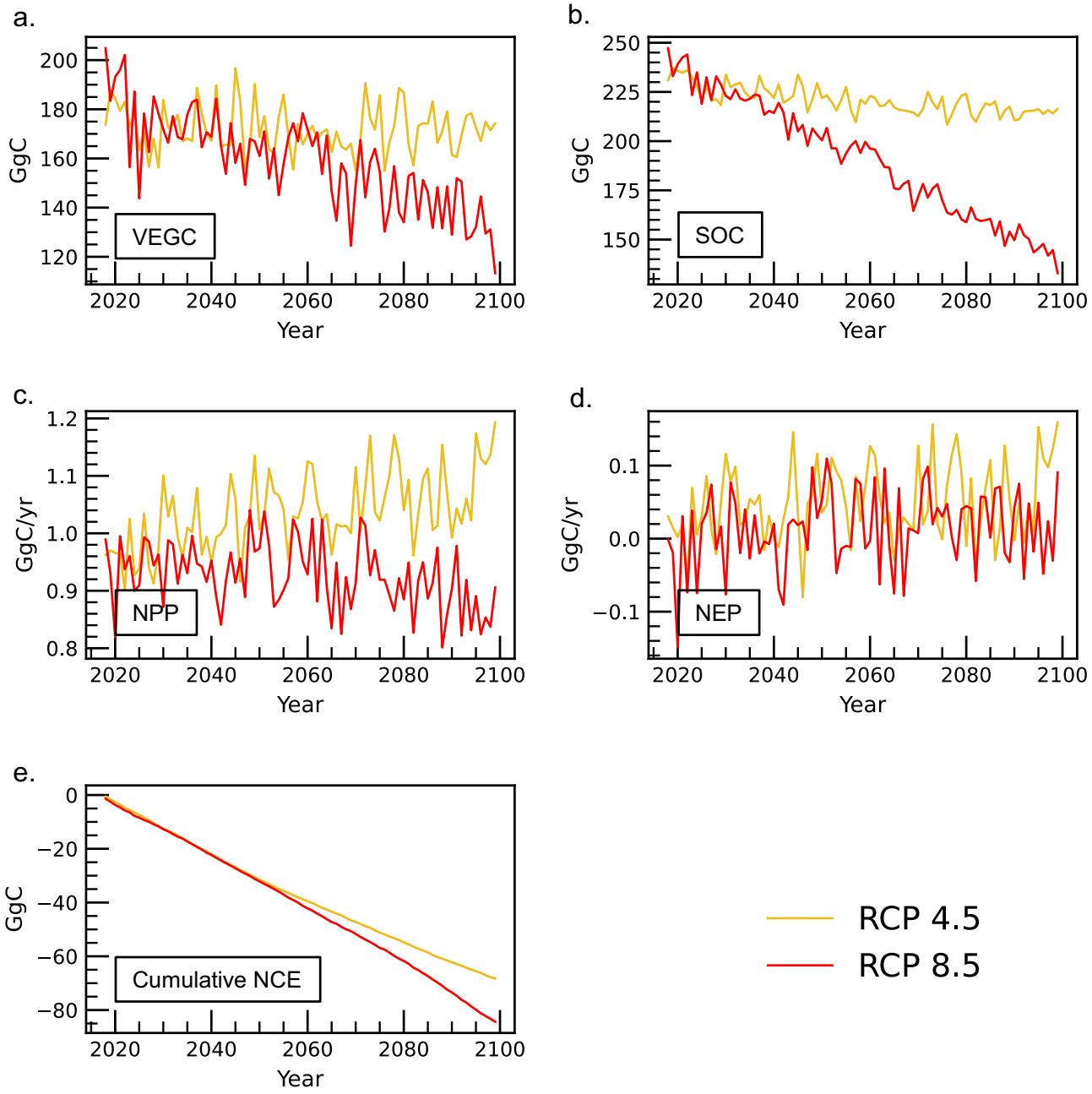

Fig. 5 | Modeled carbon stock and flux trends under RCP scenarios. a Vegetation carbon (VEGC). **b** Soil organic carbon (SOC). **c** Net primary productivity (NPP). **d** Net ecosystem productivity (NEP). **e** Cumulative net carbon exchange (NCE). The yellow line represents RCP 4.5, while the red line represents RCP 8.5. Carbon trends are statistically significant (p value < 0.05), based on the 20-models aggregation. PFTs are defined in Fig. 1.

climate change impacts on western United States biomes because forest, shrubland, and grassland biomes all play crucial roles in carbon sequestration. These results should also contribute to the broader discussions about the future of western United States biomes as carbon sinks. Further, our study highlights the need for continued research to inform effective forest and grassland management and climate change mitigation efforts. Effective planning and management can help ensure forest persistence and grassland productivity, as these two ecosystems are critical carbon sinks.

Methods

Model description and development

The Terrestrial Ecosystem Model (TEM)[43], Fig. 6, is a process-based biogeochemical model that tracks the carbon, nitrogen, and water flow between the atmosphere, vegetation, and soils[21]. The model includes photosynthesis, nitrogen uptake, respiration, litterfall, allocation, and dissolved organic carbon[44]. In addition, the model incorporates multiple structural pools for vegetation carbon and nitrogen, as well as a single pool for soil organic carbon and nitrogen and soil inorganic nitrogen (Fig. 6).

The application of the model requires input datasets from transient climates, including surface air temperature, diurnal temperature range, precipitation, solar radiation, vapor pressure, and wind speed, as well as CO_2, O_3, nitrogen deposition, and static soil texture and elevation datasets. This study adds biogeography components to the model to determine the most optimal/productive PFTs under different climatic conditions. The model is calibrated using known values of carbon fluxes (GPP, NPP, nitrogen saturated NPP), carbon stocks (vegetation and soil carbon), nitrogen fluxes (plant nitrogen uptake), nitrogen stocks (vegetation nitrogen, soil organic, and inorganic nitrogen) and evapotranspiration.

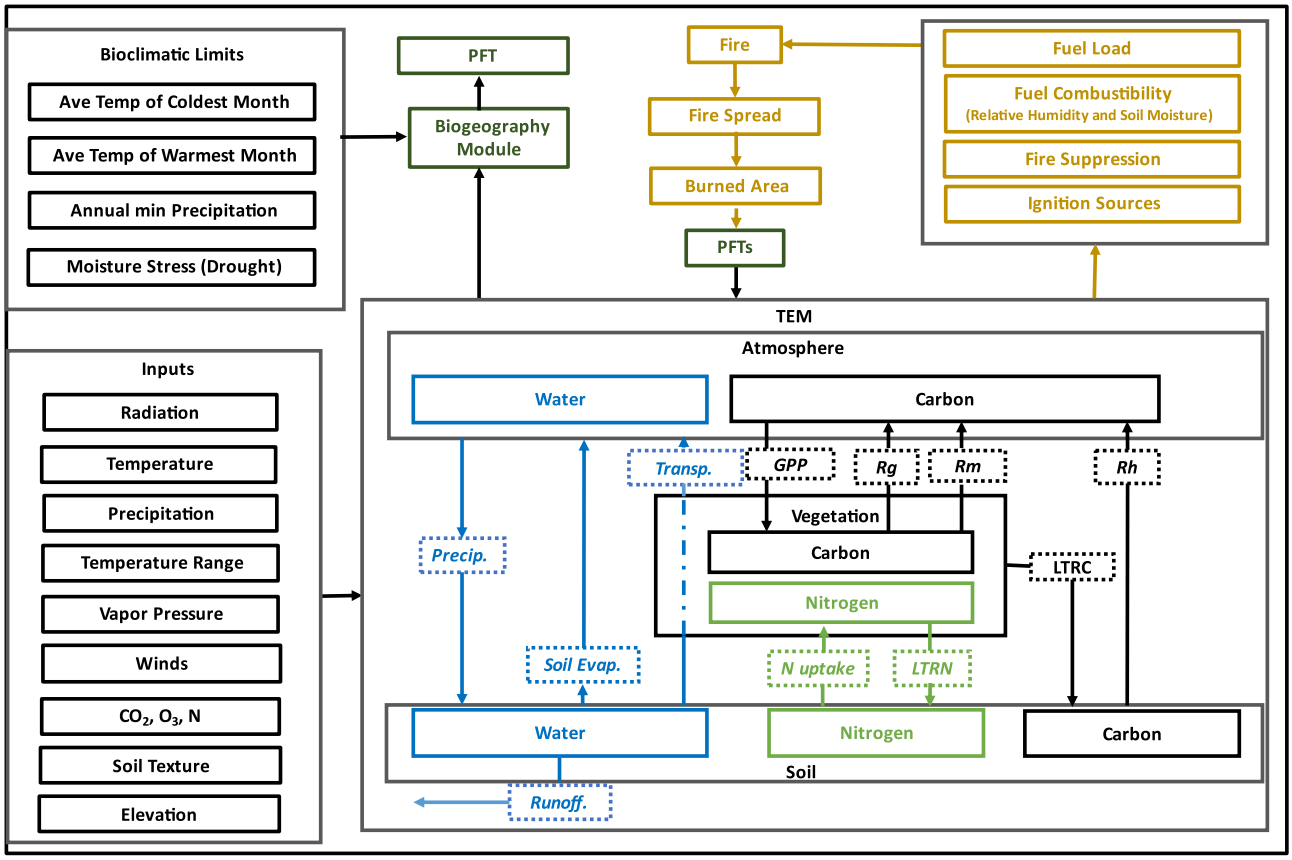

Fig. 6 | TEM model overview. Illustration of the TEM model, highlighting its components: biogeography, biochemistry, and fire.

The model includes a seed pool as one of the structural pools. During allocation, a PFT-dependent fraction of carbon and nitrogen is supplied to the seed pool from the labile pool as windfall allocation, which occurs when the size of the labile pool is larger than the available storage space of the structural pools. The labile pool itself is replenished by GPP. The allocation of resources to the seed pool is based on a cost-benefit analysis[45].

Fire module

The fire model is adapted from the Community Land Model (CLM) 5.0 and is based on fuel availability, ignition, combustibility, fire spread, and fire suppression[46,47]. Fuel load is determined from biomass (vegetation carbon). Fuel Combustibility is determined by relative humidity and soil moisture. Both natural and anthropogenic ignition sources are considered. The burned area is determined by wind speed and specific fire spread rates for each PFT, as done in CLM[46,47], and is also affected by climate, PFT composition, and human activity. The severity of the fire is determined by climate and fuel availability and is modified by the percent of the grid area burned. The fire combustion completeness factors for leaves and stems are similar to those used in CLM. The fire suppression factor is calculated based on population density[46,47].

For historical fires (1750–2014), fire return interval (FRI) from LANDFIRE is added to the CLM fire module to determine the frequency of historical fires[48,49]. The FRI layer quantifies the average period between fires under the presumed historical fire regime. In addition to these FRIs, we include periods of fire suppression or deficit in the West, i.e., ~1800s to 1980. Fire frequency and severity are modified during these periods to reflect better historical fire regimes. The fire suppression factor is also calculated as done in CLM[46,47].

While the FRI from LANDFIRE is used to govern the historical frequency of fires, the CLM module retains control over the occurrence and severity of these fires based on climate and ignition factors. Fire impact is calculated once the burned area is determined (Supplementary Notes 1).

Apart from the historical fires, which are modified to better reflect historical fire regimes, the fire module is a one-to-one implementation of the Community Land Model's non-peat fires (outside cropland and tropical closed forests). For a detailed description of the Fire Module, refer to the CLM 5.0 manual and Li et al.[46,47]. While the model may not capture all the complexities of ecological dynamics, given the grid size and the fact that we simulate vegetation at the PFT level, it offers an improvement and provides valuable insights for understanding forest change over the next century.

Biogeography module

The biogeography module uses elements from the BIOME4[19,20], which uses specified bioclimatic envelopes to determine the PFT distribution. The BIOME4 model is driven by long-term averages of monthly mean temperature, solar insolation, and precipitation. Given different climatic variables, the model predicts which PFT can occur in each grid and selects the dominant PFT depending on optimum climatic conditions (Table 1)[19,20,50,51]. Our model uses bioclimatic envelopes (Table 1) to determine the PFT that can exist in each grid cell.

The biogeography module identifies potential PFTs for each grid cell based on the bioclimatic envelopes in Table 1. From the resultant potential PFT, the PFT with the highest total NPP (above and below ground) over the preceding 30-year period was designated as the dominant type within each grid cell and assigned 100% areal coverage. The validation criteria for the biogeography module is its capacity to accurately determine the dominant PFT within each grid cell during the final 30 years of the historical run (1984–2014) (Supplementary Notes 2).

The $\frac{AET}{PET}$ is the ratio of actual evapotranspiration to potential evapotranspiration calculated using the Penman–Monteith formulation[52]. The minimum $\frac{AET}{PET}$ envelopes used in this study are estimated by modeling historical $\frac{AET}{PET}$ values in the western United States using historical climate datasets of CRU 4.5 starting from 1900 to 2014. The minimum $\frac{AET}{PET}$ threshold values are then determined by selecting the 5th percentile value for each PFT

Table 1 | Bioclimatic envelopes used in the biogeography model

Plant functional type	T_c (°C)	T_w (°C)	min P (mm/year)	min $\frac{AET}{PET}$
Boreal Forest	−60	21	200	0.60
Mixed Temperate Forest (Coniferous)	−40	24	300	0.60
Mixed Temperate Forest (Deciduous)	−10	21	750	0.60
Temperate Coniferous Forest	−40	24	300	0.60
Temperate Deciduous Forest	−10	21	750	0.60
Short Grassland	−20	35	250	0.50
Arid Shrubland	0	35	100	0.50
Xeromorphic Forest & Woodlands	−5	32	250	0.55
Temperate Broadleaf Evergreen Forest	−10	25	750	0.60

T_c mean temperature of the coldest month, T_w = mean temperature of the warmest month, min P = minimum annual minimum precipitation, and min $\frac{AET}{PET}$ = minimum moisture stress index.

during the summer months when vegetation experiences the most moisture stress. The $\frac{AET}{PET}$ ranges linearly between 1 for unstressed vegetation and 0 at the wilting point[53,54]. Environments with $\frac{AET}{PET} < 0.75$ are considered low water stress, $0.5 < \frac{AET}{PET} \leq 0.75$ moderate water stress, $0.25 < \frac{AET}{PET} \leq 0.5$ high water stress, and $\frac{AET}{PET} \leq 0.25$ severe water stress[55]. $\frac{AET}{PET}$ has been implemented in many dynamic vegetation models where it is presumed to be linearly related to net photosynthesis and, therefore, has been viewed as an integrated measure of the annual amount of growth-limiting drought stress[55].

The biogeography and fire module further extends the TEM's capabilities, enabling the simulation of biogeographical patterns and PFT distribution

Experiments and methods of analysis

Each grid cell is initially populated with a single dominant PFT, with the exception of grids containing mixed temperate forests, which comprise two PFTs (Temperate Conifers and Deciduous). While grass and shrub PFTs are present within most grids[56,57], they do not constitute the dominant PFTs. In grids where shrubs and grass PFTs do not exist, we assume seed sources of grasses and shrubs are readily available.

Two runs were done to simulate historical vegetation patterns. The first run included fire disturbance, as detailed in the preceding fire module section, while the second run was conducted without any historical fire disturbance to ascertain the influence of biomass or forest standage on the shift in dominant PFT. Both historical model runs started from a state of dynamic equilibrium without fire, following forest equilibration; the transient run spans from 1750 to 2014. At the conclusion of both historical runs, the final vegetation state is saved and utilized as the initial conditions for future runs (2015–2100).

Twenty future model runs were performed for each RCP scenario using the RCP 4.5 and RCP 8.5 general circulation models supplied by the Multivariate Adapted Constructed Analogs (MACA)[58]. The future run was initialized using the ecosystem state saved at the end of the historical run. It employed the fire routine adapted from the Community Land Model (CLM) 5.0[29], as detailed in the preceding fire module section.

For each RCP scenario, the outputs of 20 future models were aggregated. This aggregation was achieved by calculating the mean of each variable's output across all models, thus providing a central tendency measure for our projections. Our methodology is grounded in approaches similar to the IPCC, in which multi-model means are used to show a synthesis response. We also add the standard deviation to represent a measure of variance around the multi-model means. Additionally, to account for variability and uncertainties inherent in model predictions, we computed each variable's standard deviation. While this approach does not directly consider the individual model distributions, it offers a robust way to synthesize model outputs, providing a comprehensive and statistically sound overview of projected changes under different scenarios. The final calculations and statistics were performed with 100% coverage of the dominant PFT. A PFT is considered dominant if more than 10 out of the 20-models agree. The principal model output variables analyzed in this study were selected carbon stocks and fluxes: Net Primary Productivity, Vegetation Carbon, Net Ecosystem Productivity, Net Carbon Exchange, and Soil Organic Carbon. To assess temporal changes in carbon stocks and fluxes, we compared and analyzed outcomes for the future and historical runs for 1984–2014 and 2070–2100, respectively. It was observed that there was no difference in the change in dominant PFT by the end of the century when the fire was turned on or off during the historical run.

Datasets

The historical climate dataset used in this study spans from 1750 to 2014. Data from 1750 to 1900 were obtained from MPI-ESM-P[59], and data from 1900–2014 are based on the Climatic Research Unit (CRU 4.5) dataset[60]. Bias correction was performed on the CRU data using grid MET (Gridded Surface Meteorological dataset) data by Abatzoglou (2013) to accurately match the historical CRU and future MACA datasets (which were bias corrected to grid MET). This approach involved creating a delta (for temperature /ratio (for other variables) for the bias correction between grid MET and CRU, then using the grid MET fill-in values of the period 1979-2014 (the overlap period) baseline for the bias correction. The bias correction was done to eliminate any offsets between historical CRU and Future MACA climate datasets, reducing the offset between future and historical climates. The MPI-ESM-P was also bias-corrected in a similar manner to the bias-corrected CRU datasets. The two bias-corrected datasets, MPI-ESM-P and CRU were combined to produce the millennial climate dataset spanning 1750–2014.

For the projection of future climates spanning 2015 to 2100, we used the 20 Coupled Model Intercomparison Project Version 5 RCP 8.5 and 4.5 climate datasets downscaled using MACA[58]. All bias correction was applied after the datasets were all scaled to the common 0.5° × 0.5° spatial resolution (MPI downscaled and MACA upscaled) to match the resolution at which we ran TEM. All downscaled interpolations were done using the nearest neighbor approach, which assigns the value of the nearest grid in the low-resolution dataset to the grid in the high-resolution dataset while upscaling averaged the appropriate grids. Land use and land cover are based on the cohort approach developed from the Harmonized Global Land Use potential land cover datasets[61] and CO_2 values based on RCP 4.5 and 8.5[62]. Finally, data for forested grids in the western United States were extracted from these datasets for input to TEM.

Data availability

This study utilized several types of data, all of which are accessible through: 1. Population Density Data: the dataset for population density, which was integral to our study, is available for access at the following link: https://sedac.ciesin.columbia.edu/data/set/gpw-v4-population-density-rev11/data-download. 2. LISOTD Climatology Dataset: the LISOTD Climatology Dataset, which was used for Lightning data in our study, can be found at

https://ghrc.nsstc.nasa.gov/ using this link: https://ghrc.nsstc.nasa.gov/pub/lis/climatology/LIS-OTD/HRMC/data/nc/. 3. Multivariate Adaptive Constructed Analogs (MACA): the MACA data, crucial for our climatology analysis, is accessible at: https://www.climatologylab.org/maca.html. 4. Processed data used to make the figures for both RCP scenarios can be found at https://zenodo.org/records/10574102. Following the principles of open and transparent research, we have provided direct hyperlinks and unique identifiers for each dataset. These links facilitate easy access to the data for replication and further research purposes. If there are any restrictions on data access, these do not apply to the current study, as all datasets and tools used are publicly available.

Code availability

This study utilized the Terrestrial Ecosystem Model. The source code for the TEM the biogeography module, and the statistical analysis tools used in this study are publicly available on GitHub. Access to these resources can be obtained under the repository name "TEM_Biogeography" at https://github.com/Lehigh-TEM-Felzer-Lab and at https://zenodo.org/records/10476119.

Received: 27 July 2023; Accepted: 31 January 2024;
Published online: 12 February 2024

References

1. Batllori, E., Parisien, M.-A., Parks, S. A., Moritz, M. A. & Miller, C. Potential relocation of climatic environments suggests high rates of climate displacement within the North American protection network. *Glob. Change Biol.* **23**, 3219–3230 (2017).
2. Climate Change 2021: the physical science basis. Contribution of Working Group I to the Sixth Assessment Report of the Intergovernmental Panel on Climate Change. (Cambridge University Press, 2021). https://doi.org/10.1017/9781009157896.
3. Wasserman, T. N. & Mueller, S. E. Climate influences on future fire severity: a synthesis of climate-fire interactions and impacts on fire regimes, high-severity fire, and forests in the western United States. *Fire Ecol.* **19**, 43 (2023).
4. Coop, J. D. et al. Wildfire-driven forest conversion in Western North American landscapes. *BioScience* **70**, 659–673 (2020).
5. Macdonald, G. et al. Drivers of California's changing wildfires: a state-of-the-knowledge synthesis. *Int. J. Wildland Fire*, https://doi.org/10.1071/WF22155 (2023).
6. Williams, J. W. & Jackson, S. T. Novel climates, no-analog communities, and ecological surprises. *Front. Ecol. Environ.* **5**, 475–482 (2007).
7. Glover, K. C., George, J., Heusser, L. & MacDonald, G. M. West Coast vegetation shifts as a response to climate change over the past 130,000 years: geographic patterns and process from pollen data. *Phys. Geogr.* **42**, 542–560 (2021).
8. Nolan, C. et al. Past and future global transformation of terrestrial ecosystems under climate change. *Science* **361**, 920–923 (2018).
9. Whitlock, C., Shafer, S. L. & Marlon, J. The role of climate and vegetation change in shaping past and future fire regimes in the northwestern US and the implications for ecosystem management. *For. Ecol. Manag.* **178**, 5–21 (2003).
10. Finch, D. M. Climate change in grasslands, shrublands, and deserts of the interior American West: a review and needs assessment. Gen. Tech. Rep. RMRS-GTR-285 Fort Collins CO. US Dep. Agric. For. Serv. Rocky Mt. Res. Stn. 139 P **285**, (2012).
11. Overpeck, J. T., Rind, D. & Goldberg, R. Climate-induced changes in forest disturbance and vegetation. *Nature* **343**, 51–53 (1990).
12. Brown, C. D. & Johnstone, J. F. Once burned, twice shy: repeat fires reduce seed availability and alter substrate constraints on Picea mariana regeneration. *For. Ecol. Manag.* **266**, 34–41 (2012).
13. Loehman, R. A., Reinhardt, E. & Riley, K. L. Wildland fire emissions, carbon, and climate: seeing the forest and the trees – a cross-scale assessment of wildfire and carbon dynamics in fire-prone, forested ecosystems. *For. Ecol. Manag.* **317**, 9–19 (2014).
14. Westerling, A. L., Turner, M. G., Smithwick, E. A. H., Romme, W. H. & Ryan, M. G. Continued warming could transform Greater Yellowstone fire regimes by mid-21st century. *Proc. Natl. Acad. Sci.* **108**, 13165–13170 (2011).
15. Keyser, A. R., Krofcheck, D. J., Remy, C. C., Allen, C. D. & Hurteau, M. D. Simulated increases in fire activity reinforce shrub conversion in a Southwestern US forest. *Ecosystems* **23**, 1702–1713 (2020).
16. Davis, K. T. et al. Wildfires and climate change push low-elevation forests across a critical climate threshold for tree regeneration. *Proc. Natl. Acad. Sci.* **116**, 6193–6198 (2019).
17. Clark, J. A., Loehman, R. A. & Keane, R. E. Climate changes and wildfire alter vegetation of Yellowstone National Park, but forest cover persists. *Ecosphere* **8**, e01636 (2017).
18. Rehfeldt, G. E., Crookston, N. L., Warwell, M. V. & Evans, J. S. Empirical analyses of plant-climate relationships for the Western United States. *Int. J. Plant Sci.* **167**, 1123–1150 (2006).
19. Prentice, I. C. et al. Special paper: a global biome model based on plant physiology and dominance, soil properties and climate. *J. Biogeogr.* **19**, 117–134 (1992).
20. Kaplan, J. O. et al. Climate change and Arctic ecosystems: 2. modeling, paleodata-model comparisons, and future projections. *J. Geophys. Res.* **108**, 8171 (2003).
21. Felzer, B. S. Carbon, nitrogen, and water response to climate and land use changes in Pennsylvania during the 20th and 21st centuries. *Ecol. Model.* **240**, 49–63 (2012).
22. Guiterman, C. H. et al. Vegetation type conversion in the US Southwest: frontline observations and management responses. *Fire Ecol*. **18**, 6 (2022).
23. Siirila-Woodburn, E. R. et al. A low-to-no snow future and its impacts on water resources in the western United States. *Nat. Rev. Earth Environ.* **2**, 800–819 (2021).
24. Overpeck, J. T. & Udall, B. Climate change and the aridification of North America. *Proc. Natl. Acad. Sci.* **117**, 11856–11858 (2020).
25. Gergel, D. R., Nijssen, B., Abatzoglou, J. T., Lettenmaier, D. P. & Stumbaugh, M. R. Effects of climate change on snowpack and fire potential in the western USA. *Clim. Change* **141**, 287–299 (2017).
26. Xu, T., Zhang, A., Xu, X. & Jia, G. Synchronized slowdown of climate warming and carbon sink enhancement over deciduous broadleaf forests based on FLUXNET analysis. *Ecol. Indic.* **155**, 111042 (2023).
27. Sleeter, B. M. et al. Effects of 21st-century climate, land use, and disturbances on ecosystem carbon balance in California. *Glob. Change Biol.* **25**, 3334–3353 (2019).
28. Xu, C. et al. Increasing impacts of extreme droughts on vegetation productivity under climate change. *Nat. Clim. Change* **9**, 948–953 (2019).
29. Hill, A. P. & Field, C. B. Forest fires and climate-induced tree range shifts in the western US. *Nat. Commun.* **12**, 6583 (2021).
30. Davis, K. T. et al. Reduced fire severity offers near-term buffer to climate-driven declines in conifer resilience across the western United States. *Proc. Natl. Acad. Sci.* **120**, e2208120120 (2023).
31. Stevens-Rumann, C. S. & Morgan, P. Tree regeneration following wildfires in the western US: a review. *Fire Ecol.* **15**, 15 (2019).
32. Harvey, B. J., Donato, D. C. & Turner, M. G. High and dry: post-fire tree seedling establishment in subalpine forests decreases with post-fire drought and large stand-replacing burn patches. *Glob. Ecol. Biogeogr.* **25**, 655–669 (2016).
33. Perry, C. H., Finco, M. V. & Wilson, B. T. Forest Atlas of the United States. FS-1172 https://www.fs.usda.gov/treesearch/pubs/64468 (2022).
34. Falk, D. A. et al. Mechanisms of forest resilience. *For. Ecol. Manag.* **512**, 120129 (2022).
35. Coop, J. D., Parks, S. A., McClernan, S. R. & Holsinger, L. M. Influences of prior wildfires on vegetation response to subsequent fire

in a reburned Southwestern landscape. *Ecol. Appl. Publ. Ecol. Soc. Am.* **26**, 346–354 (2016).
36. Balch, J. K., Bradley, B. A., D'Antonio, C. M. & Gómez-Dans, J. Introduced annual grass increases regional fire activity across the arid western USA (1980–2009). *Glob. Change Biol.* **19**, 173–183 (2013).
37. Kellner, J. R., Kendrick, J. & Sax, D. F. High-velocity upward shifts in vegetation are ubiquitous in mountains of western North America. *PLOS Clim.* **2**, e0000071 (2023).
38. Parks, S. A., Holsinger, L. M., Miller, C. & Parisien, M.-A. Analog-based fire regime and vegetation shifts in mountainous regions of the western US. *Ecography* **41**, 910–921 (2018).
39. Bradley, B. A. Regional analysis of the impacts of climate change on cheatgrass invasion shows potential risk and opportunity. *Glob. Change Biol.* **15**, 196–208 (2009).
40. Noss, R. F., Franklin, J. F., Baker, W. L., Schoennagel, T. & Moyle, P. B. Managing fire-prone forests in the western United States. *Front. Ecol. Environ.* **4**, 481–487 (2006).
41. Beschta, R. L. et al. Postfire management in forested public lands of the western USA. *Conserv. Biol.* **18**, 957–967 (2004).
42. Allen, I., Chhin, S. & Zhang, J. Fire and forest management in montane forests of the Northwestern States and California, USA. *Fire* **2**, 17 (2019).
43. Jared M Kodero. Lehigh-TEM-Felzer-Lab/TEM_Biogeography: tem_biogeography_2024/09/01. https://doi.org/10.5281/ZENODO.10476119 (2024).
44. Felzer, B. S. & Jiang, M. Effect of land use and land cover change in context of growth enhancements in the United States since 1700: net source or sink. ? *J. Geophys. Res. Biogeosci.* **123**, 3439–3457 (2018).
45. Felzer, B. S., Cronin, T. W., Melillo, J. M., Kicklighter, D. W. & Schlosser, C. A. Importance of carbon-nitrogen interactions and ozone on ecosystem hydrology during the 21st century. *J. Geophys. Res. Biogeosci.* **114**, 2008JG000826 (2009).
46. Lawrence, D. et al. CLM5.0 technical description. (2018).
47. Li, F., Zeng, X. D. & Levis, S. A process-based fire parameterization of intermediate complexity in a dynamic global vegetation model. *Biogeosciences* **9**, 2761–2780 (2012).
48. Landfire, U. S. LANDFIRE Rapid Assessment. 2007. Rapid assessment reference condition models. https://www.fs.usda.gov/database/feis/fire_regime_table/fire_regime_table.html (2007).
49. Barrett, S. et al. Interagency fire regime condition class guidebook. Version 3.0. https://www.fs.usda.gov/database/feis/fire_regime_table/fire_regime_table.html (2010).
50. Prentice, I. C. et al. Dynamic global vegetation modeling: quantifying terrestrial ecosystem responses to large-scale environmental change. *In:* Terrestrial Ecosystems in a Changing World (eds. Canadell, J. G., Pataki, D. E. & Pitelka, L. F.) 175–192 (Springer, 2007). https://doi.org/10.1007/978-3-540-32730-1_15.
51. Zhao, D., Zhu, Y., Wu, S. & Zheng, D. Projection of vegetation distribution to 1.5 °C and 2 °C of global warming on the Tibetan Plateau. *Glob. Planet. Change* **202**, 103525 (2021).
52. Monteith, J. L. Evaporation and environment. *Symp. Soc. Exp. Biol.* **19**, 205–234 (1965).
53. Boreux, J. J., Gadbin-Henry, C., Joel, G. & Tessier, L. Radial tree-growth modelling with fuzzy regression. *Can. J. For. Res.* **28**, 1249–1260 (1998).
54. Vidale, P. L. et al. On the treatment of soil water stress in GCM simulations of vegetation physiology. *Front. Environ. Sci*. **9**, 689301 (2021).
55. Speich, M. J. R. Quantifying and modeling water availability in temperate forests: a review of drought and aridity indices. *iForest* **12**, 1–16 (2019).
56. Krebs, M. A., Reeves, M. C. & Baggett, L. S. Predicting understory vegetation structure in selected western forests of the United States using FIA inventory data. *For. Ecol. Manag.* **448**, 509–527 (2019).
57. Knapp, E. E., Weatherspoon, C. P. & Skinner, C. N. Shrub seed banks in mixed conifer forests of Northern California and the role of fire in regulating abundance. *Fire Ecol.* **8**, 32–48 (2012).
58. Abatzoglou, J. T. & Brown, T. J. A comparison of statistical downscaling methods suited for wildfire applications. *Int. J. Climatol.* **32**, 772–780 (2012).
59. Schmidt, G. A. et al. Configuration and assessment of the GISS ModelE2 contributions to the CMIP5 archive: GISS MODEL-E2 CMIP5 SIMULATIONS. *J. Adv. Model. Earth Syst.* **6**, 141–184 (2014).
60. Harris, J. P. D. & Lister, O. D. H. Updated high-resolution grids of monthly climatic observations – the CRU TS3.10 Dataset. *Int. J. Climatol.* https://rmets.onlinelibrary.wiley.com/doi/10.1002/joc.3711 (2014).
61. Hurtt, G. C. et al. Harmonization of global land use change and management for the period 850–2100 (LUH2) for CMIP6. *Geosci. Model. Dev.* **13**, 5425–5464 (2020).
62. Meinshausen, M. et al. Historical greenhouse gas concentrations for climate modelling (CMIP6). *Geosci. Model. Dev.* **10**, 2057–2116 (2017).

Acknowledgements

We would like to thank Dork Sahagian, Bob Booth, and Katie Glover for guiding this study. We also thank Colin Prentice for his helpful suggestions at the start of this project. The research was funded by Lehigh University's Earth and Environmental Science Department.

Author contributions

Jared M. Kodero was the primary contributor, responsible for developing the model, conducting comprehensive research, authoring the paper, and creating all the figures. He played a vital role throughout the project's execution. Benjamin S. Felzer, as Jared M. Kodero's thesis advisor, was pivotal in the research process. He contributed to model development, particularly in the intricacies of the TEM model, and provided expert advice in biogeochemistry. Yuning Shi enhanced the model's functionality and accuracy, offering expert advice and implementing code for moisture stress thresholds. He also contributed to manuscript editing, improving its overall quality and precision.

Competing interests

The authors declare no competing interests.

Additional information

Supplementary information The online version contains supplementary material available at https://doi.org/10.1038/s43247-024-01253-6.

Correspondence and requests for materials should be addressed to Jared M. Kodero.

Peer review information *Communications Earth & Environment* thanks the anonymous reviewers for their contribution to the peer review of this work. Primary Handling Editor: Aliénor Lavergne. A peer review file is available.